



## The derivation of bi-Maxwell distribution variables from chorus emissions detected on the ground

L. Juhász<sup>(1)</sup>, J. Lichtenberger<sup>(1,2)</sup>, Y. Omura<sup>(3)</sup>, R.H. W. Friedel<sup>(4)</sup> and M. Clilverd<sup>(5)</sup>

(1)Department of Geophysics and Space Sciences, Eötvös University, Budapest, Hungary <http://sas2.elte.hu>

(2) Geodetic and Geophysical Institute, RCAES, Sopron, Hungary

(3) Research Institute for Sustainable Humanosphere, Kyoto University, Kyoto, Japan

(4) Los Alamos National Laboratory National Security Education Center (NSEC) MS-T001, Los Alamos, NM 87545, USA

(5) British Antarctic Survey (NERC), Cambridge, UK

### Abstract

“ACHDANet” (Automatic Chorus and Hiss Detector and Analyzer Network) project is an analogy to, and additional product of the well-known AWDANet [1],[2]. Our mission is to create a monitoring system which nowcast the source population in the Radiation Belts [3] based on ground-detected chorus emissions by the AWDANet stations at  $L > L_{pp}$ . In our recent paper [4], we introduced a direct method to derive the approximate bi-Maxwellian parameters of the source population from the starting frequency and frequency sweep rate of individual chorus emissions. The chorus inversion method was tested successfully on Van Allen Probes EMFISIS and ECT-HOPE data. That chorus inversion method fulfill the requirements of a future automatic detector and analyzer system: a robust technique which inputs are spectrogram of chorus emissions recorded on the ground,  $f_{ce}$  gyrofrequency and  $f_{pe}$  plasmafrequency at the assumed source region. As a next step, the effects of propagation is under investigation. In this paper we examine the application domain of the most robust propagation model, namely, propagation with a group velocity quasi-parallel to the magnetic field. In this model we apply an empirical density model [5] for plasmatrough and the critical frequency of F2 region  $f_{oF2}$  for ionosphere. We present the first results of Van Allen Probes EMFISIS and AWDANet chorus emissions which were simultaneously detected and analyzed.

### 1. Introduction

The nonlinear wave growth theory for chorus emissions was proposed by [6] and [7]. They found direct connection between the frequency sweep rate of an individual chorus emission and the density of its source population at the equatorial region. That relationship enables us to develop the above mentioned chorus inversion method. The nonlinear theory of Omura assumed that the nonlinear phase is triggered by a preceding (both in time and frequency) linear phase. It

should be noted that they describe the source population with a bi-Maxwellian distribution function, we did as well. The source population’s bi-Maxwellian distribution function has three parameters: thermal velocity parallel and perpendicular to the background magnetic field, and the density itself. The latter one can be derived from the nonlinear theory, but we need extra information for the thermal velocities. To estimate the parallel and the minimum perpendicular thermal velocities, we use the model of relativistic linear growth-rate of R-mode plasma waves [8].

Their theory affirm that chorus emissions are generated at the source region, from which they initially propagate with group-velocity and quasi-parallel to the magnetic background. A gap is formed at  $0.5 f_{ce}$  by nonlinear wave damping via Landau resonance [9] during their slightly oblique propagation away from the magnetic equator. As a consequence of the propagation, wave amplitude undergoes convective growth, while frequency sweep rate evolves in space.

### 2. Chorus inversion method

The inversion method consists of two phases (Figure 1). First we estimate the parallel and minimum perpendicular thermal velocity of the source population using the relativistic solution of electromagnetic R-mode wave instability of [8] (1 st phase blue box in Fig.1). Here we identify the band of whistler-mode waves corresponding to the linear wave growth. Assuming arbitrary energetic electron density,  $N_h$ , we search for those parallel momentum  $U_{\parallel}$  value, that produces the maximum linear growth rate at the mean frequency of the linear wave growth band. In the knowledge of  $U_{\parallel}$ , a minimum estimate for perpendicular thermal velocity  $V_{\perp 0}$  can be calculated.

Using these thermal velocities, a direct estimation of  $N_h/N_c$  is obtained from the frequency sweep rate of a chorus emission using nonlinear wave growth theory (2nd phase, blue box):

$$\tilde{\omega}_{ph} = \omega_{pe} \left( \frac{N_h}{N_c} \right)^{1/2} = \sqrt{\frac{\partial \omega}{\partial t} \frac{\pi^{5/2} \tau}{0.324 Q} \frac{\tilde{U}_{t\parallel}}{\tilde{V}_g} \exp\left(\frac{\gamma^2 \tilde{V}_R^2}{2 \tilde{U}_{t\parallel}^2}\right) \frac{\gamma}{\tilde{V}_{\perp 0} X}},$$

where  $\tilde{V}_R$  is the normalized, relativistic resonance velocity;  $\tilde{U}_{t\parallel}$  is the normalized, parallel thermal momentum;  $\tilde{V}_{\perp 0}$  is the normalized, average perpendicular velocity;  $\tilde{V}_g$  is the normalized groupvelocity;  $\gamma$  is the Lorentz-factor;  $\tau$  is the ratio of nonlinear transition time and nonlinear trapping period;  $Q$  is the depth of the electron hole.

Here, we replaced the wave amplitude  $\Omega_w$  with the optimum amplitude  $\Omega_{opt}$  in order to obtain  $N_h$ . For this study, the inputs are gyrofrequency  $\Omega_e$ , plasma frequency  $\omega_{pe}$ , frequency sweep rate of an individual chorus emission  $\partial\omega/\partial t$  and the mean frequency of the assumed band of linear growth  $\omega_{rm}$ , all from electromagnetic wave measurements (red boxes on Fig.1).

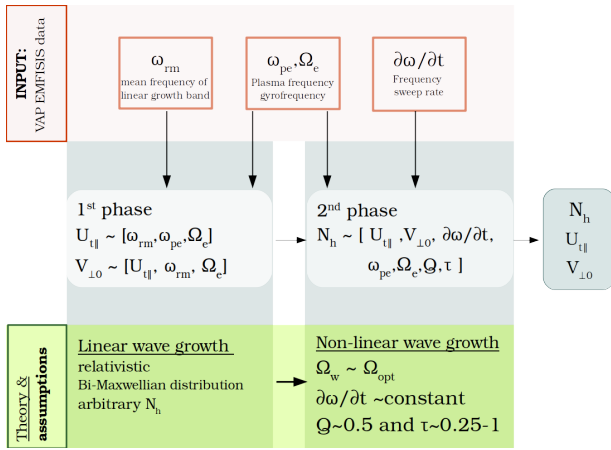


Figure 1: Chorus-inversion method: Inputs are from wave measurements (red boxes) only. As the first step, thermal momentum  $U_{t\parallel}$  and average perpendicular velocity  $V_{\perp 0}$  are calculated. The second phase is governed by non-linear wave growth. For the calculation of  $N_h$ , we use the output of the first phase,  $U_{t\parallel}$  and  $V_{\perp 0}$ . At the end of the process, we obtain the bi-Maxwellian function parameters of energetic electrons responsible for chorus emission generation. In the green boxes we note some important assumptions.

### 3. Propagation from the source region to the ground

The propagation path of whistler mode chorus waves recorded on the ground is not fully known. Based on the following empirical studies, we can build a robust model suitable for real-time automatic analysis.

The generation takes place at the magnetic equator, the chorus wave start to propagate from there and undergo frequency dependent dispersion during the propagation. As a result, the frequency sweep rate of chorus elements recorded on the ground differ from the original one, and has to be corrected to get back the equatorial frequency

sweep rate. The wave propagation model consists of three sections:

1. propagation from the origin to the top of the ionosphere (magnetospheric part);
2. propagation through ionosphere;
3. propagation from the ionospheric exit point to the receiver in the Earth-Ionosphere waveguide.

There was a consensus until recently that whistler mode waves observed on the ground propagate in ducts – density enhancement, depletion or sharp gradient. The evidence of ducts are still indirect [10], but active measurement on IMAGE satellite [11] exhibit evidences of field aligned density irregularities, both inside and outside of the plasmopause. Ground VLF transmitter signals recorded on board the Demeter and Van Allen Probes propagate mostly along the field lines in ducted mode [12]

The study of [13] opened the possibility of non-ducted propagation through inverse 3D ray-tracing calculations. These calculations always led to two major conclusions: a) the wave normal angle of the wave at the origin is large, often 90 degrees; b) the plasmopause locations were within  $+0.6L - -0.3L$  range of the receiver. The conclusion a) is in direct contradiction with the latest theory of chorus generation [7], as the generated waves start to propagate along the field line with wave normal parallel to the magnetic field. Thus the non-ducted propagation may be excluded from the model. Conclusion b), however in accordance with the standard ducted propagation scenario: a whistler mode wave packets can be recorded within 800-1000km radius of the ionospheric exit point. As field aligned density irregularities outside the plasmopause are found in IMAGE measurements, thus ducted propagation outside the plasmopause cannot be excluded. However from the long history of whistlers recorded on the ground complemented our recent studies using our AWDANet observations show very low percentage of non-plasmaspheric propagation. The only feasible propagation path thus the plasmopause itself. This is in accordance with the found close vicinity of the plasmopause during ground observation (conclusion b) above), with the theoretical considerations that the plasmopause sharp density gradient can act as a guiding structure [10], and with experimental evidences of knee whistlers [14]. The chorus waves generated at the magnetic equator start to propagate along the field line with wave normal parallel to the magnetic field. However – if no density duct along the field line – the wave propagation start to deviate from the field line quickly due to the gradient in the magnetic field and electron density. Therefore we assumed the following propagation scenario in the magnetosphere: a. the chorus waves are generated at the equator, near the plasmopause and start to propagate along the field line; b. as the magnetic field and density gradient alter the wave direction, the waves diverted toward the plasmopause are trapped by the steep density gradient and guided along the plasmopause (field line), if their wavenormal angles fall into the trapping cone. In the ionospheric path, the standard model (horizontally layered model) is used with scattering assumption, that is

at the top of the ionosphere, the power density of the ducted energy is more-or-less independent of wave normal direction in the duct due to the small irregularities in the refractive index. The wave energy leaks through the transmission cone to the Earth-Ionosphere waveguide.

The magnetospheric part was described with the model used in whistler inversion [2] and in fractional inversion of VLF transmitter signals [12]. Here, we applied [5] field aligned density distribution model as it is valid both for plasmasphere and plasmatrough. In the development and validation of the chorus propagation model, we used in-situ cold electron density measurements from Van Allen Probes.

#### 4. Validation of the inversion method using ground based and ins-situ wave and ins-situ particle measurements.

To validate our chorus inversion method on ground based recordings, we were searching for simultaneous chorus events, both recorded by AWDANet and VAP. This step is the most difficult one as satellite measurements are sporadic, both in time and space: we needed burst mode data from EMFISIS instrument, this measuring mode is rare due to the limited on board memory and telemetry capacity; the satellite passes sporadically over the ground receiver location. We found a simultaneous chorus event on 31 March 15 at 23:19:35 (Figure 2.) recorded by the EMFISIS instrument on Van Allen Probes (Figure 4) and 1 seconds later by AWDANet station Halley (Figure 3.). The ground-based chorus waves were recorded at Halley, Antarctica ( $\lambda=-75.6$  deg,  $\phi=-26.6$  deg,  $L=4.5$ ), Van Allen Probes position was at MLAT= -1.11; MLON= 35.69; MLT = 20.541; L = 5.612.



Figure 2: The magnetic footprints of VAP-A and -B close to Halley Station, Antarctica at 23:19:34.5 on 31 March 2015

First step of the validation was to remove the propagation effects using the chorus wave propagation model described in Section 3. to obtain the  $d\omega/dt$  at the source region (magnetic equator). In the next step, the chorus inversion method of [4] was applied on the in-situ and ‘backpropagated’ ground chorus element. The results are compared with the energetic electron density  $N_h$  derived from in-situ HOPE particle measurements (Table 1) in the resonant energy range of 8-11 keV.

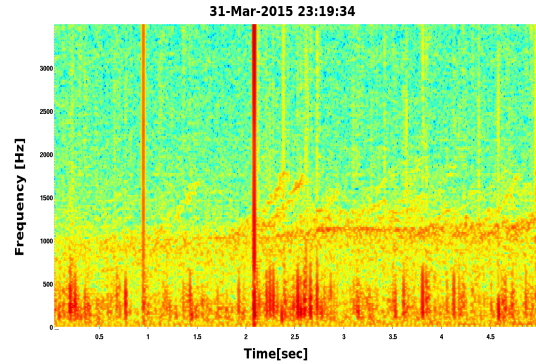


Figure 3: AWDANet recording at 23:19:36 on 31 March 2015. Two chorus emissions are visible between 2 and 2.5 sec 1000-2000 Hz

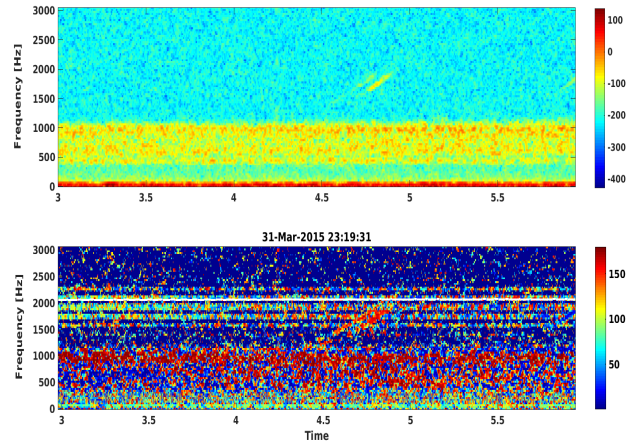


Figure 4: VAP-A EMFISIS recording at 23:19:35 on 31 March 2015. A very similar pair of choruses are visible between 4.5 and 5 sec 1000-2000 Hz. Bottom panel shows the Poynting theta, quasi-parallel propagation with red.

	HOPE particle data	EMFISIS chorus inversion	AWDANet chorus inversion
$N_h/n_c$ , $\tau=1$	0.0006 $\pm 0.0002$	0.0018 $\pm 0.0004$	0.0013 $\pm 0.0003$
$N_h/n_c$ , $\tau=0.5$	0.0006 $\pm 0.0002$	0.0004 $\pm 0.0001$	0.0003 $\pm 0.0001$

## 5. Conclusion

We can conclude that the very first example of simultaneously recorded chorus emissions showing excellent agreement. We should note that the chorus inversion of in-situ and ground-based data have slightly different results, despite of the fact that we used the most basic propagation model. However, HOPE data show much lower -still in the error range – density data. We should take into account that the comparison with HOPE particle measurements has many challenges:

1. only 4 energy channels provided the HOPE density in the resonant energy range
2. it is hard to decide which state of wave-particle interaction is reflected on the particle data
3. a more precise way would be to select HOPE data in pitch angle too, however, the lack of sufficient data points made no big differences

Our future plan is to extend our data base, searching for more examples in different times and spacecrafts.

## 5. Acknowledgements

This work was supported by Hungarian National Research, Development and Innovation Office (Grant Numbers: NN116408, NN116446 ), the JSPS KAKENHI (Grant Numbers: 15H05815, 17H06140 ) and NASA (Grant Number: NAS5-01072). The first author thanks for the Vela Fellowship provided by Los Alamos National Laboratory.

## 7. References

- [1] Lichtenberger J, Ferencz C, Bodnár L, Hamar D, Steinbach P. Automatic whistler detector and analyzer system: Automatic whistler detector, *Journal of Geophysical Research: Space Physics*, 2008 Dec 1;113(A12), doi:10.1029/2008JA013467
- [2] Lichtenberger J, Ferencz C, Hamar D, Steinbach P, Rodger CJ, Clilverd MA, Collier AB. Automatic Whistler Detector and Analyzer system: Implementation of the analyzer algorithm, *Journal of Geophysical Research: Space Physics*, 2010 Dec 1;115(A12), doi: 10.1029/2010JA015931
- [3] Jaynes, A. N., et al. ( 2015), Source and seed populations for relativistic electrons: Their roles in radiation belt changes, *J. Geophys. Res. Space Physics*, 120, 7240– 7254, doi:10.1002/2015JA021234.
- [4] Juhász, L., Omura, Y., Lichtenberger, J., & Friedel, R. H. W. (2019). Evaluation of plasma properties from chorus waves observed at the generation region. *Journal of Geophysical Research: Space Physics*, 124, 4125–4136. <https://doi.org/10.1029/2018JA026337>
- [5] Denton, R. E., J. D. Menietti, J. Goldstein, S. L. Young, and R. R. Anderson (2004), Electron density in the magnetosphere, *J. Geophys. Res.*, 109, A09215, doi:10.1029/2003JA010245.
- [6] Omura Y, Katoh Y, Summers D. “Theory and simulation of the generation of whistler-mode chorus,” *Journal of Geophysical Research: Space Physics*, 2008 Apr 1;113(A4), doi:10.1029/2007JA012622
- [7] Omura Y, Nunn D. Triggering process of whistler mode chorus emissions in the magnetosphere, *Journal of Geophysical Research: Space Physics*, 2011 May 1;116(A5), doi:10.1029/2010JA016280
- [8] Xiao, F., Thorne, R. and Summers, D. (1998). Instability of electromagnetic R-mode waves in a relativistic plasma. *Physics of Plasmas*, 5(7), pp.2489-2497.
- [9] Hsieh, Y. and Omura, Y. (2018). Nonlinear Damping of Oblique Whistler Mode Waves Via Landau Resonance. *Journal of Geophysical Research: Space Physics*, 123(9), pp.7462-7472.
- [10] Helliwell, R. A. (1965). *Whistlers and related ionospheric phenomena* (Vol. 50, p. 406). Stanford, Calif.: Stanford University Press.
- [11] Carpenter, D. (2002). Small-scale field-aligned plasmaspheric density structures inferred from the Radio Plasma Imager on IMAGE. *Journal of Geophysical Research*, 107(A9).
- [12] Koroncay, D., Lichtenberger, J., Juhász, L., Steinbach, P., & Hospodarsky, G. B. (2018). VLF transmitters as tools for monitoring the plasmasphere. *Journal of Geophysical Research: Space Physics*, 123. <https://doi.org/10.1029/2018JA025802>
- [13] Golden, D., Spasojevic, M., Foust, F., Lehtinen, N., Meredith, N. and Inan, U. (2010). Role of the plasmopause in dictating the ground accessibility of ELF/VLF chorus. *Journal of Geophysical Research: Space Physics*, 115(A11), p.n/a-n/a.
- [14] Carpenter, D. (1963). Whistler evidence of a ‘knee’ in the magnetospheric ionization density profile. *Journal of Geophysical Research*, 68(6), pp.1675-1682.